

Fundamentals of Geophysics

Second Edition

WILLIAM LOWRIE

Swiss Federal Institute of Technology, Zürich



CAMBRIDGE
UNIVERSITY PRESS

(SG)
OC 804
.L67
2007
C.2

CAMBRIDGE UNIVERSITY PRESS

Cambridge, New York, Melbourne, Madrid, Cape Town, Singapore, São Paulo

Cambridge University Press

The Edinburgh Building, Cambridge CB2 8RU, UK

Published in the United States of America by Cambridge University Press, New York

www.cambridge.org

Information on this title: www.cambridge.org/9780521675963

© W. Lowrie 2007

This publication is in copyright. Subject to statutory exception
and to the provisions of relevant collective licensing agreements,
no reproduction of any part may take place without
the written permission of Cambridge University Press.

First published 2007

Printed in United Kingdom at the University Press, Cambridge

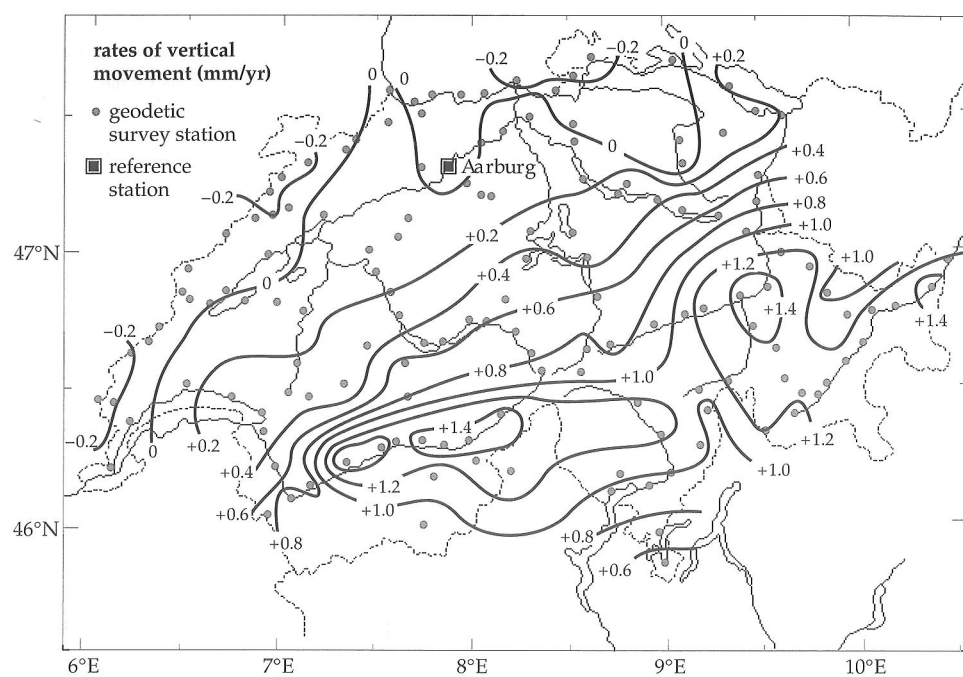
A catalog record for this publication is available from the British Library

ISBN-13 978-0-521-85902-8 hardback

ISBN-13 978-0-521-67596-3 paperback

Cambridge University Press has no responsibility for the persistence or
accuracy of URLs for external or third-party websites referred to
in this publication, and does not guarantee that any content on such
websites is, or will remain, accurate or appropriate

Fig. 2.68 Rates of vertical crustal motion in Switzerland deduced from repeated precise levelling. Broken contour lines indicate areas in which geodetic data are absent or insufficient. Positive rates correspond to uplift, negative rates to subsidence (data source: Gubler, 1991).



The rates of relative vertical movement in northeastern Switzerland are smaller than the confidence limits on the data and may not be significant, but the general tendency suggests subsidence. This region is characterized by mainly positive isostatic anomalies. The rates of vertical movement in the southern part of Switzerland exceed the noise level of the measurements and are significant. The most notable characteristic of the recent crustal motions is vertical uplift of the Alpine part of Switzerland relative to the central plateau and Jura mountains. The Alpine uplift rates are up to 1.5 mm yr^{-1} , considerably smaller than the rates observed in Fennoscandia. The most rapid uplift rates are observed in the region where isostatic anomalies are negative. The constant erosion of the mountain topography relieves the crustal load and the isostatic response is uplift. However, the interpretation is complicated by the fact that compressive stresses throughout the Alpine region acting on deep-reaching faults can produce non-isostatic uplift of the surface. The separation of isostatic and non-isostatic vertical crustal movements in the Alps will require detailed and exact information about the structure of the lithosphere and asthenosphere in this region.

Provided the applied stress does not exceed the yield stress (or elastic limit) the short-term behavior is elastic. This means that any deformation caused by the stress is completely recoverable when the stress is removed, leaving no permanent change in shape. However, if the applied stress exceeds the yield stress, the solid may experience either brittle or ductile deformation.

Brittle deformation consists of rupture without other distortion. This is an abrupt process that causes faulting in rocks and earthquakes, accompanied by the release of elastic energy in the form of seismic waves. Brittle fracture occurs at much lower stresses than the intrinsic strength of a crystal lattice. This is attributed to the presence of cracks, which modify the local internal stress field in the crystal. Fracture occurs under either extension or shear. Extensional fracture occurs on a plane at right angles to the direction of maximum tension. Shear fracture occurs under compression on one of two complementary planes which, reflecting the influence of internal friction, are inclined at an angle of less than 45° (typically about 30°) to the maximum principal compression. Brittle deformation is the main mechanism in tectonic processes that involve the uppermost 5–10 km of the lithosphere.

Ductile deformation is a slow process in which a solid acquires strain (i.e., it changes shape) over a long period of time. A material may react differently to a stress that is applied briefly than to a stress of long duration. If it experiences a large stress for a long period of time a solid can slowly and permanently change shape. The time-dependent deformation is called plastic flow and the capacity of the solid to flow is called its *ductility*. The ductility of a solid above its yield stress depends on temperature and confining pressure, and materials that are brittle under ordinary conditions may be ductile at high temperature and pressure. The behavior of rocks and minerals in

2.8 RHEOLOGY

2.8.1 Brittle and ductile deformation

Rheology is the science of the deformation and flow of solid materials. This definition appears at first sight to contradict itself. A solid is made up of particles that cohere to each other; it is rigid and resists a change of shape. A fluid has no rigidity; its particles can move about comparatively freely. So how can a solid flow? In fact, the way in which a solid reacts to stress depends on how large the stress is and the length of time for which it is applied.

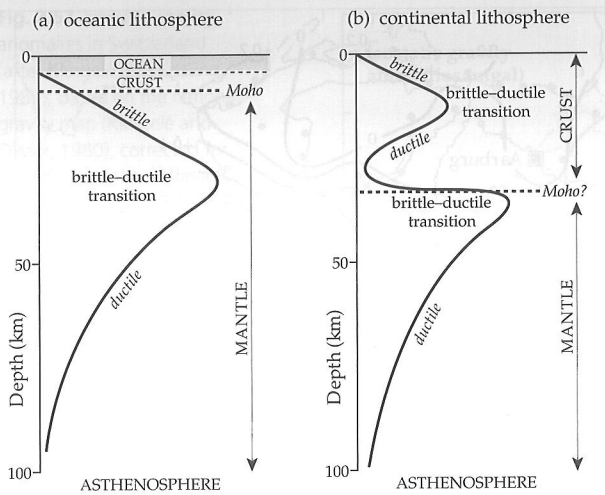


Fig. 2.69 Hypothetical vertical profiles of rigidity in (a) oceanic lithosphere and (b) continental lithosphere with the estimated depths of brittle–ductile transitions (after Molnar, 1988).

the deep interior of the Earth is characterized by ductile deformation.

The transition from brittle to ductile types of deformation is thought to occur differently in oceanic and continental lithosphere (Fig. 2.69). The depth of the transition depends on several parameters, including the composition of the rocks, the local geothermal gradient, initial crustal thickness and the strain rate. Consequently it is sensitive to the vertically layered structure of the lithosphere. The oceanic lithosphere has a thin crust and shows a gradual increase in strength with depth, reaching a maximum in the upper mantle at about 30–40 km depth. At greater depths the lithosphere gradually becomes more ductile, eventually grading into the low-rigidity asthenosphere below about 100 km depth. The continental crust is much thicker than the oceanic crust and has a more complex layering. The upper crust is brittle, but the minerals of the lower crust are weakened by high temperature. As a result the lower crust becomes ductile near to the Moho at about 30–35 km depth. In the upper mantle the strength increases again, leading to a second brittle–ductile transition at about 40–50 km depth. The difference in rheological layering of continental and oceanic lithosphere is important in collisions between plates. The crustal part of the continental lithosphere may detach from the mantle. The folding, underthrusting and stacking of crustal layers produce folded mountain ranges in the suture zone and thickening of the continental crust. For example, great crustal thicknesses under the Himalayas are attributed to underthrusting of crust from the Indian plate beneath the crust of the Eurasian plate.

2.8.2 Viscous flow in liquids

Consider the case when a liquid or gas flows in thin layers parallel to a flat surface (Fig. 2.70). The *laminar flow* exists as long as the speed stays below a critical value,

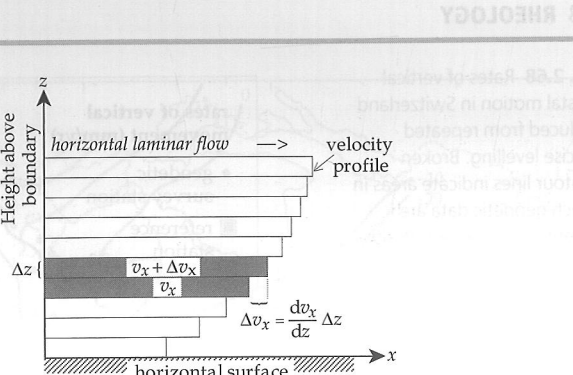


Fig. 2.70 Schematic representation of laminar flow of a fluid in infinitesimally thin layers parallel to a horizontal surface.

above which the flow becomes turbulent. Turbulent flow does not interest us here, because the rates of flow in solid earth materials are very slow.

Suppose that the velocity of laminar flow along the horizontal x -direction increases with vertical height z above the reference surface. The molecules of the fluid may be regarded as having two components of velocity. One component is the velocity of flow in the x -direction, but in addition there is a random component with a variable velocity whose root-mean-square value is determined by the temperature (Section 4.2.2). Because of the random component, one-sixth of the molecules in a unit volume are moving upward and one-sixth downward on average at any time. This causes a transfer of molecules between adjacent layers in the laminar flow. The number of transfers per second depends on the size of the random velocity component, i.e., on temperature. The influx of molecules from the slower-moving layer reduces the momentum of the faster-moving layer. In turn, molecules transferred downward from the faster-velocity layer increase the momentum of the slower-velocity layer. This means that the two layers do not move freely past each other. They exert a shear force – or drag – on each other and the fluid is said to be *viscous*.

The magnitude of the shear force F_{xz} (Section 3.2) depends on how much momentum is transferred from one layer to the next. If all the molecules in a fluid have the same mass, the momentum transfer is determined by the change in the velocity v_x between the layers; this depends on the vertical gradient of the flow velocity (dv_x/dz). The momentum exchange depends also on the number of molecules that cross the boundary between adjacent layers and so is proportional to the surface area, A . We can bring these observations together, as did Newton in the seventeenth century, and derive the following proportionality relationship for F_{xz} :

$$F_{xz} \propto A \frac{dv_x}{dz} \quad (2.110)$$

If we divide both sides by the area A , the left side becomes the shear stress σ_{xz} . Introducing a proportionality constant η we get the equation

$$\sigma_{xz} = \eta \frac{dv_x}{dz} \quad (2.111)$$

2.8 RHEOLOGY

This equation is Newton's law of viscous flow and η is the *coefficient of viscosity*. If η is constant, the fluid is called a *Newtonian fluid*. The value of η depends on the transfer rate of molecules between layers and so on temperature. Substituting the units of stress (pascal) and velocity gradient ($(\text{ms}^{-1})/\text{m} = \text{s}^{-1}$) we find that the unit of η is a pascal-second (Pa s). A shear stress applied to a fluid with low viscosity causes a large velocity gradient; the fluid flows easily. This is the case in a gas (η in air is of the order 2×10^{-5} Pa s) or in a liquid (η in water is 1.005×10^{-3} Pa s at 20 °C). The same shear stress applied to a very viscous fluid (with a large value of η) produces only a small velocity gradient transverse to the flow direction. The layers in the laminar flow are reluctant to move past each other. The viscous fluid is “sticky” and it resists flow. For example, η in a viscous liquid like engine oil is around 0.1–10 Pa s, three or four orders of magnitude higher than in water.

2.8.3 Flow in solids

The response of a solid to an applied load depends upon whether the stress exceeds the elastic limit (Section 3.2.1) and for how long it is applied. When the yield stress (elastic limit) is reached, a solid may deform continuously without further increase in stress. This is called *plastic deformation*. In *perfectly plastic* behavior the stress-strain curve has zero slope, but the stress-strain curves of plastically deformed materials usually have a small positive slope (see Fig. 3.2a). This means that the stress must be increased above the yield stress for plastic deformation to advance. This effect is called *strain-hardening*. When the stress is removed after a material has been strain-hardened, a permanent residual strain is left.

Consider the effects that ensue if a stress is suddenly applied to a material at time t_0 , held constant until time t_1 and then abruptly removed (Fig. 2.71a). As long as the applied stress is lower than the yield stress, the solid deforms elastically. The elastic strain is acquired immediately and remains constant as long as the stress is applied. Upon removal of the stress, the object at once recovers its original shape and there is no permanent strain (Fig. 2.71b).

If a constant load greater than the yield stress is applied, the resulting strain consists of a constant elastic strain and a changing *plastic* strain, which increases with time. After removal of the load at t_1 the plastic deformation does not disappear but leaves a permanent strain (Fig. 2.71c). In some plastic materials the deformation increases slowly at a decreasing rate, eventually reaching a limiting value for any specific value of the stress. This is called *viscoelastic* deformation (Fig. 2.71d). When the load is removed at t_1 , the elastic part of the deformation is at once restored, followed by a slow decrease of the residual strain. This phase is called *recovery* or *delayed elasticity*. Viscoelastic behavior is an important rheological process deep in the Earth, for example in the asthenosphere and deeper mantle.

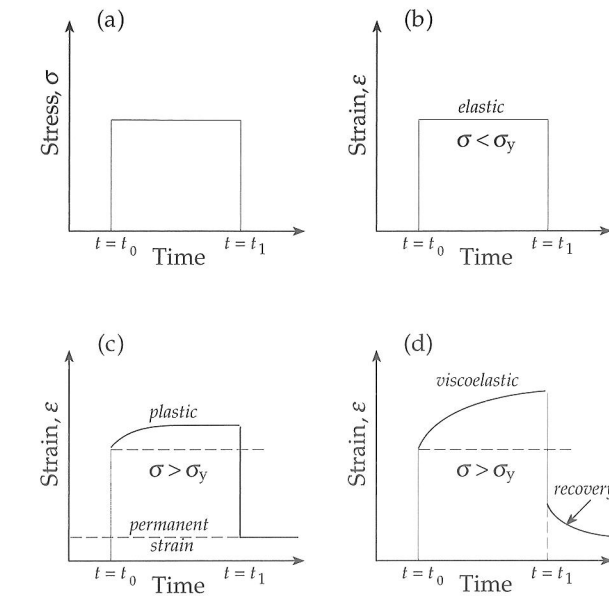


Fig. 2.71 (a) Application of a constant stress σ to a solid between times t_0 and t_1 ; (b) variation of elastic strain below the yield point; (c) plastic strain and (d) viscoelastic deformation at stresses above the yield point σ_y .

The analogy to the viscosity of liquids is apparent by inspection of Eq. (2.111). Putting $v_x = dx/dt$ and changing the order of differentiation, the equation becomes

$$\sigma_{xz} = \eta \frac{d}{dz} \frac{dx}{dt} = \eta \frac{d}{dt} \frac{dx}{dz} = \eta \frac{d}{dt} \varepsilon_{xz} \quad (2.112)$$

This equation resembles the elastic equation for shear deformation, which relates stress and strain through the shear modulus (see Eq. (3.16)). However, in the case of the “viscous flow” of a solid the shear stress depends on the strain rate. The parameter η for a solid is called the *viscosity modulus*, or *dynamic viscosity*. It is analogous to the viscosity coefficient of a liquid but its value in a solid is many orders of magnitude larger. For example, the viscosity of the asthenosphere is estimated to be of the order of 10^{20} – 10^{21} Pa s. Plastic flow in solids differs from true flow in that it only occurs when the stress exceeds the yield stress of the solid. Below this stress the solid does not flow. However, internal defects in a metal or crystal can be mobilized and reorganized by stresses well below the yield stress. As a result the solid may change shape over a long period of time.

2.8.3.1 Viscoelastic model

Scientists have tried to understand the behavior of rocks under stress by devising models based on mechanical analogs. In 1890 Lord Kelvin modelled viscoelastic deformation by combining the characteristics of a perfectly elastic solid and a viscous liquid. An applied stress causes both elastic and viscous effects. If the elastic strain is ε , the corresponding elastic part of the stress is $E\varepsilon$, where E is Young's modulus (Section 3.2.4). Similarly, if the rate of change of strain with time is $d\varepsilon/dt$, the viscous part of

the applied stress is $\eta \frac{d\epsilon}{dt}$, where η is the viscosity modulus. The applied stress σ is the sum of the two parts and can be written

$$\sigma = E\epsilon + \eta \frac{d\epsilon}{dt} \quad (2.113)$$

To solve this equation we first divide throughout by E , then define the *retardation time* $\tau = \eta/E$, which is a measure of how long it takes for viscous strains to exceed elastic strains. Substituting and rearranging the equation we get

$$\epsilon + \tau \frac{d\epsilon}{dt} = \frac{\sigma}{E} \quad (2.114)$$

$$\frac{\epsilon}{\tau} + \frac{d\epsilon}{dt} = \frac{\epsilon_m}{\tau} \quad (2.115)$$

where $\epsilon_m = \sigma/E$. Multiplying throughout by the integrating factor $e^{t/\tau}$ gives

$$\frac{\epsilon}{\tau} e^{t/\tau} + \frac{d\epsilon}{dt} e^{t/\tau} = \frac{\epsilon_m}{\tau} e^{t/\tau} \quad (2.116)$$

$$\frac{d}{dt}(\epsilon e^{t/\tau}) = \frac{\epsilon_m}{\tau} e^{t/\tau} \quad (2.117)$$

Integrating both sides of this equation with respect to t gives

$$\epsilon e^{t/\tau} = \epsilon_m e^{t/\tau} + C \quad (2.118)$$

where C is a constant of integration determined by the boundary conditions. Initially, the strain is zero, i.e., at $t=0, \epsilon=0$; substituting in Eq. (2.118) gives $C=\epsilon_m$. The solution for the strain at time t is therefore

$$\epsilon = \epsilon_m(1 - e^{-t/\tau}) \quad (2.119)$$

The strain rises exponentially to a limiting value given by $\epsilon_m = \sigma/E$. This is characteristic of viscoelastic deformation.

2.8.4 Creep

Many solid materials deform slowly at room temperature when subjected to small stresses well below their brittle strength for long periods of time. The slow time-dependent deformation is known as *creep*. This is an important mechanism in the deformation of rocks because of the great intervals of time involved in geological processes. It is hard enough to approximate the conditions of pressure and temperature in the real Earth, but the time factor is an added difficulty in investigating the phenomenon of creep in laboratory experiments.

The results of observations on rock samples loaded by a constant stress typically show three main regimes of creep (Fig. 2.72a). At first, the rock at once strains elastically. This is followed by a stage in which the strain initially increases rapidly (i.e., the strain rate is high) and then levels off. This stage is known as *primary creep* or *delayed elastic creep*. If the stress is removed within this regime, the deformation drops rapidly as the elastic strain recovers, leaving a

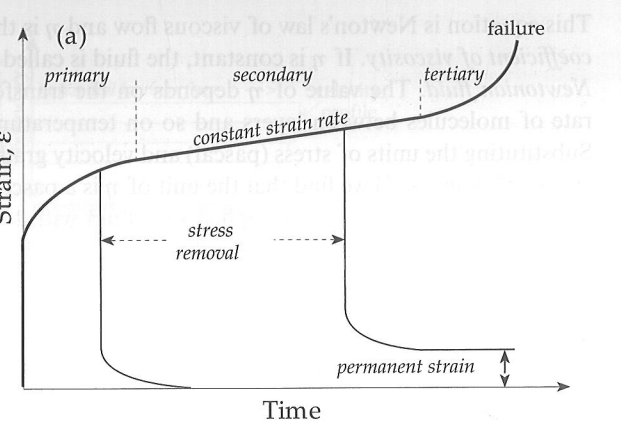


Fig. 2.72 Hypothetical strain-time curve for a material exhibiting creep under constant stress, and (b) model creep curve that combines elastic, viscoelastic and viscous elements (after Ramsay, 1967).

deformation that sinks progressively to zero. Beyond the primary stage creep progresses at a slower and nearly constant rate. This is called *secondary creep* or *steady-state creep*. The rock deforms plastically, so that if the stress is removed a permanent strain is left after the elastic and delayed elastic recoveries. After the secondary stage the strain rate increases ever more rapidly in a stage called *tertiary creep*, which eventually leads to failure.

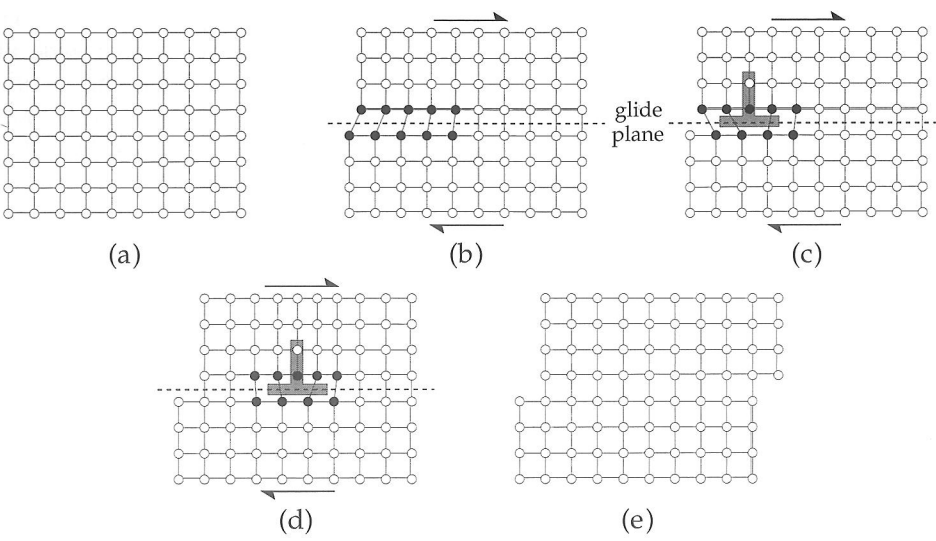
The primary and secondary stages of the creep curve can be modelled by combining elastic, viscoelastic and viscous elements (Fig. 2.72b). Below the yield stress only elastic and delayed elastic (viscoelastic) deformation occur and the solid does not flow. The strain flattens off at a limiting value $\epsilon_m = \sigma/E$. The viscous component of strain rises linearly with time, corresponding to a constant strain rate. In practice the stress must exceed the yield stress σ_y for flow to occur. In this case the viscous component of strain is proportional to the excess stress ($\sigma - \sigma_y$) and to the time t . Combining terms gives the expression

$$\epsilon = \frac{\sigma}{E} + \epsilon_m(1 - e^{-t/\tau}) + \frac{(\sigma - \sigma_y)}{\eta} t \quad (2.120)$$

This simple model explains the main features of experimentally observed creep curves. It is in fact very difficult to ensure that laboratory observations are representative of creep in the Earth. Conditions of pressure and temperature

2.8 RHEOLOGY

Fig. 2.73 Permanent (plastic) shear deformation produced by motion of a dislocation through a crystal in response to shear stress: (a) undeformed crystal lattice, (b) entry of dislocation at left edge, (c) accommodation of dislocation into lattice, (d) passage of dislocation across the crystal, and (e) sheared lattice after dislocation leaves the crystal.



in the crust and upper mantle can be achieved or approximated. The major problems arise from the differences in timescales and creep rates. Even creep experiments conducted over months or years are far shorter than the lengths of time in a geological process. The creep rates in nature (e.g., around 10^{-14} s^{-1}) are many orders of magnitude slower than the slowest strain rate used in laboratory experiments (around 10^{-8} s^{-1}). Nevertheless, the experiments have provided a better understanding of the rheology of the Earth's interior and the physical mechanisms active in different depths.

2.8.4.1 Crystal defects

Deformation in solids does not take place homogeneously. Laboratory observations on metals and minerals have shown that crystal defects play an important role. The atoms in a metal or crystal are arranged regularly to form a lattice with a simple symmetry. In some common arrangements the atoms are located at the corners of a cube or a hexagonal prism, defining a *unit cell* of the crystal. The lattice is formed by stacking unit cells together. Occasionally an imperfect cell may lack an atom. The space of the missing atom is called a *vacancy*. Vacancies may be distributed throughout the crystal lattice, but they can also form long chains called *dislocations*.

There are several types of dislocation, the simplest being an *edge dislocation*. It is formed when an extra plane of atoms is introduced in the lattice (Fig. 2.73). The edge dislocation terminates at a plane perpendicular to it called the *glide plane*.

It clearly makes a difference if the extra plane of atoms is above or below the glide plane, so edge dislocations have a sign. This can be represented by a T-shape, where the cross-bar of the T is parallel to the glide plane and the stalk is the extra plane of atoms. If oppositely signed edge dislocations meet, they form a complete plane of atoms and the dislocations annihilate each other. The displacement of atoms in the vicinity of a dislocation increases the local internal stress in the crystal. As a result,

the application of a small external stress may be enough to mobilize the dislocation, causing it to glide through the undisturbed part of the crystal (Fig. 2.73). If the dislocation glide is not blocked by an obstacle, the dislocation migrates out of the crystal, leaving a shear deformation.

Another common type of dislocation is the *screw dislocation*. It also is made up of atoms that are displaced from their regular positions, in this case forming a spiral about an axis.

The deformation of a crystal lattice by dislocation glide requires a shear stress; hydrostatic pressure does not cause plastic deformation. The shear stress needed to actuate dislocations is two or three orders of magnitude less than the shear stress needed to break the bonds between layers of atoms in a crystal. Hence, the mobilization of dislocations is an important mechanism in plastic deformation at low stress. As deformation progresses it is accompanied by an increase in the dislocation density (the number of dislocations per unit area normal to their lengths). The dislocations move along a glide plane until it intersects the glide plane of another set of dislocations. When several sets of dislocations are mobilized they may interfere and block each other, so that the stress must be increased to mobilize them further. This is manifest as strain-hardening, which is a thermodynamically unstable situation. At any stage of strain-hardening, given enough time, the dislocations redistribute themselves to a configuration with lower energy, thereby reducing the strain. The time-dependent strain relaxation is called *recovery*.

Recovery can take place by several processes, each of which requires thermal energy. These include the annihilation of oppositely signed edge dislocations moving on parallel glide planes (Fig. 2.74a) and the climb of edge dislocations past obstacles against which they have piled up (Fig. 2.74b). Edge dislocations with the same sign may align to form walls between domains of a crystal that have low dislocation density (Fig. 2.74c), a process called polygonization. These are some of the ways in which thermal energy promotes the migration of lattice defects,

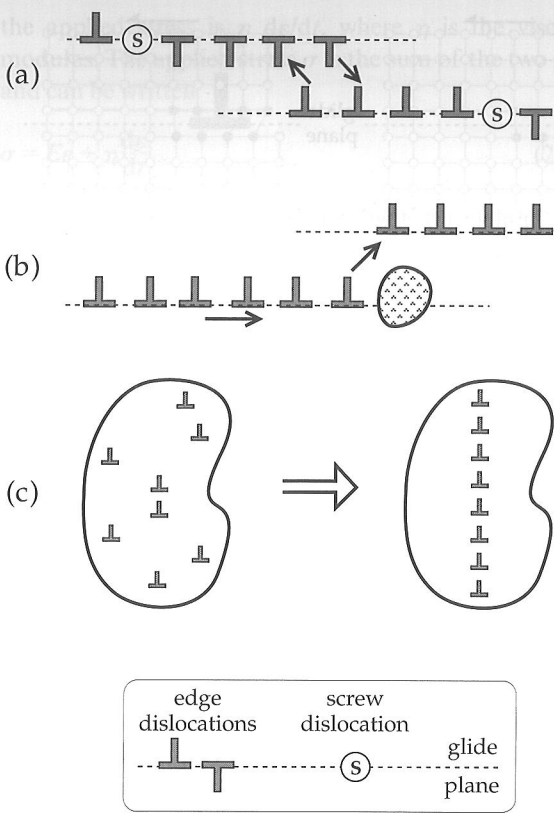


Fig. 2.74 Thermally activated processes that assist recovery: (a) annihilation of oppositely signed edge dislocations moving on parallel glide planes, (b) climb of edge dislocations past obstacles, and (c) polygonization by the alignment of edge dislocations with the same sign to form walls separating regions with low dislocation density (after Ranalli, 1987).

eventually driving them out of the crystal and leaving an annealed lattice.

2.8.4.2 Creep mechanisms in the Earth

Ductile flow in the Earth's crust and mantle takes place by one of three mechanisms: low-temperature plastic flow; power-law creep; or diffusion creep. Each mechanism is a thermally activated process. This means that the strain rate depends on the temperature T according to an exponential function with the form $e^{-E_a/kT}$. Here k is Boltzmann's constant, while E_a is the energy needed to activate the type of flow; it is called the *activation energy*. At low temperatures, where $T \ll E_a/k$, the strain rate is very slow and creep is insignificant. Because of the exponential function, the strain rate increases rapidly with increasing temperature above $T = E_a/k$. The type of flow at a particular depth depends on the local temperature and its relationship to the melting temperature T_{mp} . Above T_{mp} the interatomic bonds in the solid break down and it flows as a true liquid.

Plastic flow at low temperature takes place by the motion of dislocations on glide planes. When the dislocations encounter an internal obstacle or a crystal boundary they pile up and some rearrangement is necessary.

The stress must be increased to overcome the obstacle and reactivate dislocation glide. Plastic flow can produce large strains and may be an important mechanism in the bending of the oceanic lithosphere near some subduction zones. It is likely to be most effective at depths below the brittle–ductile transition.

Power-law creep, or hot creep, also takes place by the motion of dislocations on glide planes. It occurs at higher temperatures than low-temperature plastic flow, so internal obstacles to dislocation migration are thermally activated and diffuse out of the crystal as soon as they arise. The strain rate in power-law creep is proportional to the n th power of the stress σ and has the form

$$\frac{d\epsilon}{dt} = A \left(\frac{\sigma}{\mu} \right)^n e^{-E_a/kT} \quad (2.121)$$

where μ is the rigidity modulus and A is a constant with the dimensions of strain rate; typically $n \geq 3$. This relationship means that the strain rate increases much more rapidly than the stress. From experiments on metals, power-law creep is understood to be the most important mechanism of flow at temperatures between $0.55T_{mp}$ and $0.85T_{mp}$. The temperature throughout most of the mantle probably exceeds half the melting point, so power-law creep is probably the flow mechanism that permits mantle convection. It is also likely to be the main form of deformation in the lower lithosphere, where the relationship of temperature to melting point is also suitable.

Diffusion creep consists of the thermally activated migration of crystal defects in the presence of a stress field. There are two main forms. *Nabarro–Herring creep* consists of diffusion of defects through the body of a grain; *Coble creep* takes place by migration of the defects along grain boundaries. In each case the strain rate is proportional to the stress, as in a Newtonian fluid. It is therefore possible to regard ductile deformation by diffusion creep as the slow flow of a very viscous fluid. Diffusion creep has been observed in metals at temperatures $T > 0.85T_{mp}$. In the Earth's mantle the temperature approaches the melting point in the asthenosphere. As indicated schematically in Fig. 2.69 the transition from the rigid lithosphere to the soft, viscous underlying asthenosphere is gradational. There is no abrupt boundary, but the concept of rigid lithospheric plates moving on the soft, viscous asthenosphere serves well as a geodynamic model.

2.8.5 Rigidity of the lithosphere

Lithospheric plates are thin compared to their horizontal extents. However, they evidently react rigidly to the forces that propel them. The lithosphere does not easily buckle under horizontal stress. A simple analogy may be made to a thin sheet of paper resting on a flat pillow. If pushed on one edge, the page simply slides across the pillow without crumpling. Only if the leading edge encounters an obstacle does the page bend, buckling upward some distance in

2.8 RHEOLOGY

front of the hindrance, while the leading edge tries to burrow under it. This is what happens when an oceanic lithospheric plate collides with another plate. A small forebulge develops on the oceanic plate and the leading edge bends downward into the mantle, forming a subduction zone.

The ability to bend is a measure of the rigidity of the plate. This is also manifest in its reaction to a local vertical load. If, in our analogy, a small weight is placed in the middle of the page, it is pressed down into the soft pillow. A large area around the weight takes part in this process, which may be compared with the Vening Meinesz type of regional isostatic compensation (Section 2.7.2.3). The weight of a seamount or chain of islands has a similar effect on the oceanic lithosphere. By studying the flexure due to local vertical loads, information is obtained about a *static property* of the lithosphere, namely its resistance to bending.

In our analogy the locally loaded paper sheet would not bend if it lay on a hard flat table. It is only able to flex if it rests on a soft, yielding surface. After the weight is removed, the page is restored to its original flat shape. The restoration after unloading is a measure of the properties of the pillow as well as the page. A natural example is the rebound of regions (such as the Canadian shield or Fennoscandia) that have been depressed by now-vanished ice-sheets. The analysis of the rates of glacial rebound provides information about a *dynamic property* of the mantle beneath the lithosphere. The depression of the surface forces mantle material to flow away laterally to make way for it; when the load is removed, the return mantle flow presses the concavity back upward. The ease with which the mantle material flows is described by its dynamic viscosity.

The resistance to bending of a thin elastic plate overlying a weak fluid is expressed by an elastic parameter called the *flexural rigidity* and denoted D . For a plate of thickness h ,

$$D = \frac{E}{12(1-\nu^2)} h^3 \quad (2.122)$$

where E is Young's modulus and ν is Poisson's ratio (see Sections 3.2.3 and 3.2.4 for the definition of these elastic constants). The dimensions of E are Nm^{-2} and ν is dimensionless; hence, the dimensions of D are those of a bending moment (N m). D is a fundamental parameter of the elastic plate, which describes how easily it can be bent; a large value of D corresponds to a stiff plate.

Here we consider two situations of particular interest for the rigidity of the oceanic lithosphere. The first is the bending of the lithosphere by a topographic feature such as an oceanic island or seamount; only the vertical load on the elastic plate is important. The second is the bending of the lithosphere at a subduction zone. In this case vertical and horizontal forces are located along the edge of the plate and the plate experiences a bending moment which deflects it downward.

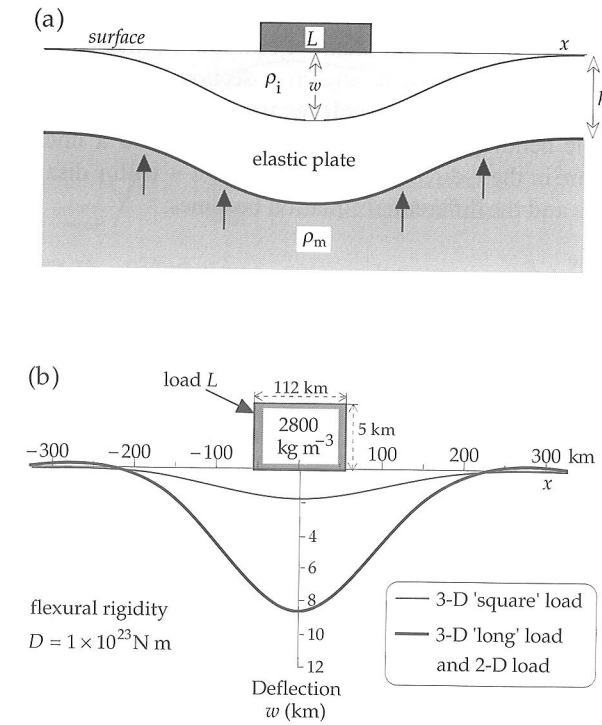


Fig. 2.75 (a) Geometry for the elastic bending of a thin plate of thickness h supported by a denser substratum: the surface load L causes a downward bending w . (b) Comparison of 2D and 3D elastic plate models. The load is taken to be a topographic feature of density 2800 kg m^{-3} , height 5 km and cross-sectional width 112 km (after Watts et al., 1975).

2.8.5.1 Lithospheric flexure caused by oceanic islands

The theory for elastic bending of the lithosphere is derived from the bending of thin elastic plates and beams. This involves a fourth-order differential equation, whose derivation and solution are beyond the scope of this book. However, it is instructive to consider the forces involved in setting up the equation, and to examine its solution in a simplified context.

Consider the bending of a thin isotropic elastic plate of thickness h carrying a surface load $L(x, y)$ and supported by a substratum of density ρ_m (Fig. 2.75a). Let the deflection of the plate at a position (x, y) relative to the center of the load be $w(x, y)$. Two forces act to counteract the downward force of the load. The first, arising from Archimedes' principle, is a buoyant force equal to $(\rho_m - \rho_i)gw$, where ρ_i is the density of the material that fills in the depression caused by the deflection of the plate. The second force arises from the elasticity of the beam. Elasticity theory shows that this produces a restoring force proportional to a fourth-order differential of the deflection w . Balancing the elastic and buoyancy forces against the deforming load leads to the equation

$$D \left[\frac{\partial^4 w}{\partial x^4} + 2 \frac{\partial^4 w}{\partial x^2 \partial y^2} + \frac{\partial^4 w}{\partial y^4} \right] + (\rho_m - \rho_i)gw = L(x, y) \quad (2.123)$$

For a linear topographic feature, such as a mountain range, oceanic island or chain of seamounts, the bending geometry is the same in any cross-section normal to its length and the problem reduces to the two-dimensional elastic bending of a thin beam. If the load is a linear feature in the y -direction, the variation of w with y disappears and the differential equation becomes:

$$D \frac{\partial^4 w}{\partial x^4} + (\rho_m - \rho_i) g w = L \quad (2.124)$$

An important example is a linear load L concentrated along the y -axis at $x=0$. The solution is a damped sinusoidal function:

$$w = w_0 e^{-x/\alpha} \left(\cos \frac{x}{\alpha} + \sin \frac{x}{\alpha} \right) \quad (2.125)$$

where w_0 is the amplitude of the maximum deflection underneath the load (at $x=0$). The parameter α is called the *flexural parameter*; it is related to the flexural rigidity D of the plate by

$$\alpha^4 = \frac{4D}{(\rho_m - \rho_i)g} \quad (2.126)$$

The elasticity of the plate (or beam) distributes the load of the surface feature over a large lateral distance. The fluid beneath the load is pushed aside by the penetration of the plate. The buoyancy of the displaced fluid forces it upward, causing uplift of the surface adjacent to the central depression. Equation (2.125) shows that this effect is repeated with increasing distance from the load, the wavelength of the fluctuation is $\lambda = 2\pi\alpha$. The amplitude of the disturbance diminishes rapidly because of the exponential attenuation factor. Usually it is only necessary to consider the central depression and the first uplifted region. The wavelength λ is equal to the distance across the central depression. Substituting in Eq. (2.126) gives D , which is then used with the parameters E and v in Eq. (2.122) to obtain h , the thickness of the elastic plate. The computed values of h are greater than the thickness of the crust, i.e., the elastic plate includes part of the upper mantle. The value of h is equated with the thickness of the elastic lithosphere.

The difference between the deflection caused by a two-dimensional load (i.e., a linear feature) and that due to a three-dimensional load (i.e., a feature that has limited extent in the x - and y -directions) is illustrated in Fig. 2.75b. If the length of the three-dimensional load normal to the cross-section is more than about ten times its width, the deflection is the same as for a two-dimensional load. A load with a square base (i.e., extending the same distance along both x - and y -axes) causes a central depression that is less than a quarter the effect of the linear load.

The validity of the lithospheric flexural model of isostasy can be tested by comparing the computed gravity effect of the model with the observed free-air gravity anomaly Δg_F . The isostatic compensation of the Great Meteor seamount in the North Atlantic provides a suitable test for a three-dimensional model (Fig. 2.76). The

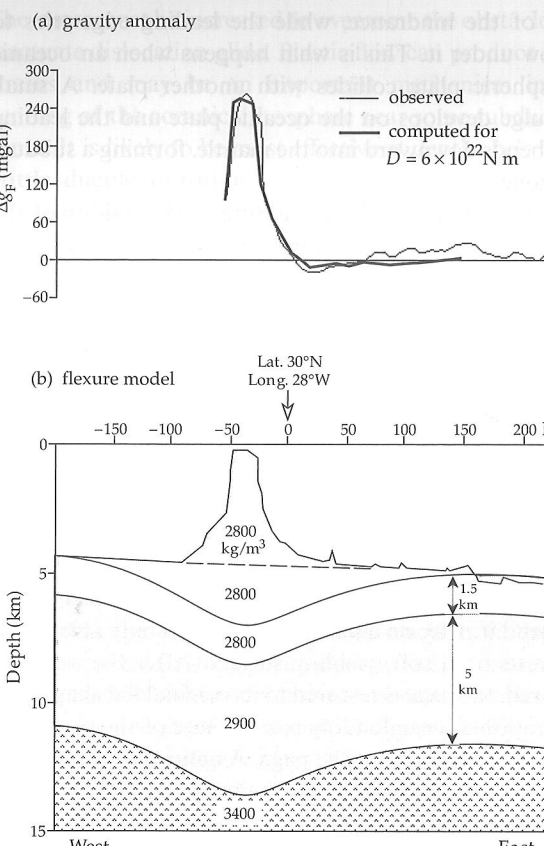


Fig. 2.76 (a) Comparison of observed free-air gravity anomaly profile across the Great Meteor seamount with the anomaly computed for (b) a lithospheric flexure model of isostatic compensation (after Watts *et al.*, 1975).

shape of the free-air gravity anomaly obtained from detailed marine gravity surveys was found to be fitted best by a model in which the effective flexural rigidity of the deformed plate was assumed to be 6×10^{22} N m.

2.8.5.2 Lithospheric flexure at a subduction zone

The bathymetry of an oceanic plate at a subduction zone is typified by an oceanic trench, which can be many kilometers deep (Fig. 2.77a). Seaward of the trench axis the plate develops a small upward bulge (the outer rise) which can extend for 100–150 km away from the trench and reach heights of several hundred meters. The lithospheric plate bends sharply downward in the subduction zone. This bending can also be modelled with a thin elastic plate.

In the model, a horizontal force P pushes a plate of thickness h toward the subduction zone, the leading edge carries a vertical load L , and the plate is bent by a bending moment M (Fig. 2.77b). The horizontal force P is negligible in comparison to the effects of M and L . The vertical deflection of the plate must satisfy Eq. (2.124), with the same parameters as in the previous example. Choosing the origin to be the point nearest the trench where the deflection is zero simplifies the form of the solution, which is

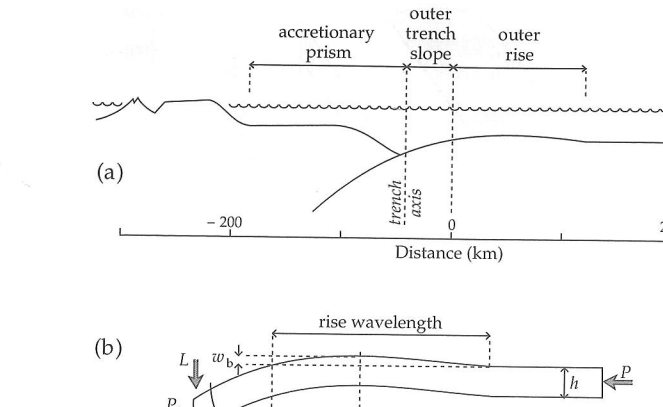


Fig. 2.77 (a) Schematic structural cross-section at a subduction zone (after Caldwell and Turcotte, 1979), and (b) the corresponding thin-plate model (after Turcotte *et al.*, 1978).

$$w = Ae^{-x/\alpha} \sin \frac{x}{\alpha} \quad (2.127)$$

where A is a constant and α is the flexural parameter as in Eq. (2.126). The value of the constant A is found from the position x_b of the forebulge, where $dw/dx = 0$:

$$\frac{dw}{dx} = A \left\{ -\frac{1}{\alpha} e^{-x/\alpha} \sin \frac{x}{\alpha} + \frac{1}{\alpha} e^{-x/\alpha} \cos \frac{x}{\alpha} \right\} = 0 \quad (2.128)$$

from which

$$x_b = \frac{\pi}{4} \alpha \quad \text{and} \quad A = w_b \sqrt{2} e^{\pi/4} \quad (2.129)$$

It is convenient to normalize the horizontal distance and vertical displacement: writing $x' = x/x_b$ and $w' = w/w_b$, the generalized equation for the elastic bending at an oceanic trench is obtained:

$$w' = \sqrt{2} \sin \left(\frac{\pi}{4} x' \right) \exp \left[\frac{\pi}{4} (1 - x') \right] \quad (2.130)$$

The theoretical deflection of oceanic lithosphere at a subduction zone obtained from the elastic bending model agrees well with the observed bathymetry on profiles across oceanic trenches (Fig. 2.78a, b). The calculated thicknesses of the elastic lithosphere are of the order 20–30 km and the flexural rigidity is around 10^{23} N m. However, at some trenches the assumption of a completely elastic upper lithosphere is evidently inappropriate. At the Tonga trench the model curve deviates from the observed bathymetry inside the trench (Fig. 2.78c). It is likely that the elastic limit is exceeded at parts of the plate where the curvature is high. These regions may yield, leading to a reduction in the effective rigidity of the plate. This effect can be taken into account by assuming that the inelastic deformation is perfectly plastic. The deflection calculated within the trench for an elastic-perfectly plastic model agrees well with the observed bathymetry.

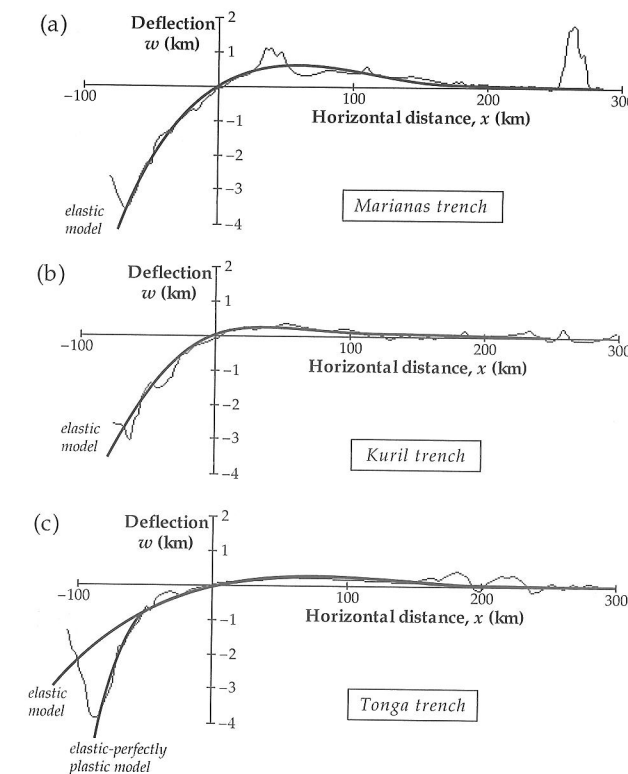


Fig. 2.78 Observed (solid) and theoretical (dashed) bathymetric profiles for elastic flexure of the lithosphere at (a) the Marianas trench and (b) the Kuril trench. The flexure at (c) the Tonga trench is best explained by an elastic-perfectly plastic model (after Turcotte *et al.*, 1978).

2.8.5.3 Thickness of the lithosphere

The rheological response of a material to stress depends on the duration of the stress. The reaction to a short-lasting stress, as experienced during the passage of a seismic wave, may be quite different from the reaction of the same material to a steady load applied for a long period of time. This is evident in the different thicknesses obtained for the lithosphere in seismic experiments and in elastic plate modelling. Long-period surface waves penetrate well into the upper mantle. Long wavelengths are slowed down by the low rigidity of the asthenosphere, so the dispersion of surface waves allows estimates of the seismic thickness of the lithosphere. For oceanic lithosphere the seismic thickness increases with age of the lithosphere (i.e., with distance from the spreading center), increasing to more than 100 km at ages older than 100 Ma (Fig. 2.79). The lithospheric thicknesses obtained from elastic modelling of the bending caused by seamounts and island chains or at subduction zones also increase with distance from the ridge, but are only one-third to one-half of the corresponding seismic thickness. The discrepancy shows that only the upper part of the lithosphere is elastic. Indeed, if the entire lithosphere had the flexural rigidity found in elastic models ($D \approx 10^{21}$ – 10^{23} N m), it would bend by only small amounts under topographic loads or at subduction zones. The base of the elastic lithosphere agrees well with the modelled depths of the 300–600 °C oceanic isotherms. At greater

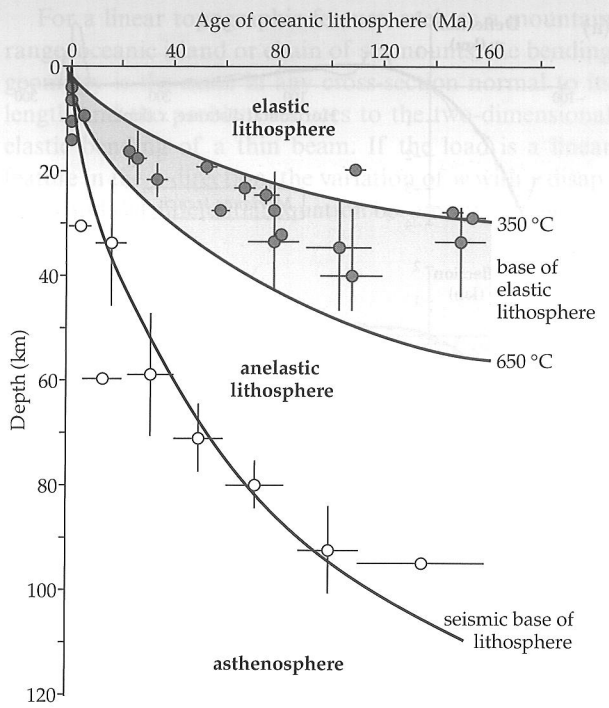


Fig. 2.79 Seismic and elastic thicknesses of oceanic lithosphere as a function of age (after Watts *et al.*, 1980).

depths the increase in temperature results in anelastic behavior of the lower lithosphere.

The elastic thickness of the continental lithosphere is much thicker than that of the oceanic lithosphere, except in rifts, passive continental margins and young orogenic belts. Precambrian shield areas generally have a flexural thickness greater than 100 km and a high flexural rigidity of around 10^{25} N m. Rifts, on the other hand, have a flexural thickness less than 25 km. Both continental and oceanic lithosphere grade gradually into the asthenosphere, which has a much lower rigidity and is able to flow in a manner determined by mantle viscosity.

2.8.6 Mantle viscosity

As illustrated by the transition from brittle to ductile behavior (Section 2.8.1), the Earth's rheology changes with depth. The upper part of the lithosphere behaves elastically. It has a constant and reversible response to both short-term and long-term loads. The behavior is characterized by the rigidity or shear modulus μ , which relates the strain to the applied shear stress and so has the dimensions of stress ($N\ m^{-2}$, or Pa). The resistance of the lithosphere to flexure is described by the flexural rigidity D , which has the dimensions of a bending moment (N m). In a subduction zone the tight bending may locally exceed the elastic limit, causing parts of the plate to yield.

The deeper part of the lithosphere does not behave elastically. Although it has an elastic response to abrupt stress changes, it reacts to long-lasting stress by ductile flow. This kind of rheological behavior also characterizes the asthenosphere and the deeper mantle. Flow takes

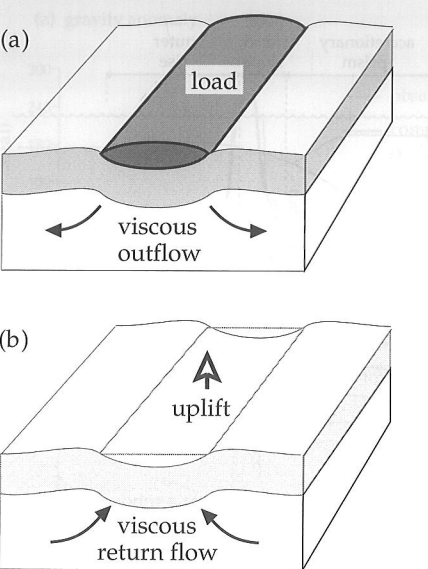


Fig. 2.80 (a) Depression of the lithosphere due to a surface load (ice-sheet) and accompanying viscous outflow in the underlying mantle; (b) return flow in the mantle and surface uplift after removal of the load.

place with a strain rate that is proportional to the stress or a power thereof. In the simplest case, the deformation occurs by Newtonian flow governed by a viscosity coefficient η , whose dimensions (Pa s) express the time-dependent nature of the process.

Under a surface load, such as an ice-sheet, the elastic lithosphere is pushed down into the viscous mantle (Fig. 2.80a). This causes an outflow of mantle material away from the depressed region. When the ice-sheet melts, removing the load, hydrostatic equilibrium is restored and there is a return flow of the viscous mantle material (Fig. 2.80b). Thus, in modelling the time-dependent reaction of the Earth to a surface load at least two and usually three layers must be taken into account. The top layer is an elastic lithosphere up to 100 km thick; it has infinite viscosity (i.e., it does not flow) and a flexural rigidity around 5×10^{24} N m. Beneath it lies a low-viscosity "channel" 75–250 km thick that includes the asthenosphere, with a low viscosity of typically 10^{19} – 10^{20} Pa s. The deeper mantle which makes up the third layer has a higher viscosity around 10^{21} Pa s.

Restoration of the surface after removal of a load is accompanied by uplift, which can be expressed well by a simple exponential relaxation equation. If the initial depression of the surface is w_0 , the deflection $w(t)$ after time t is given by

$$w(t) = w_0 e^{-t/\tau} \quad (2.131)$$

Here τ is the relaxation time, which is related to the mantle viscosity η by

$$\tau = \frac{4\pi}{\rho_m g \lambda} \eta \quad (2.132)$$

where ρ_m is the mantle density, g is gravity at the depth of the flow and λ is the wavelength of the depression, a

2.8 RHEOLOGY

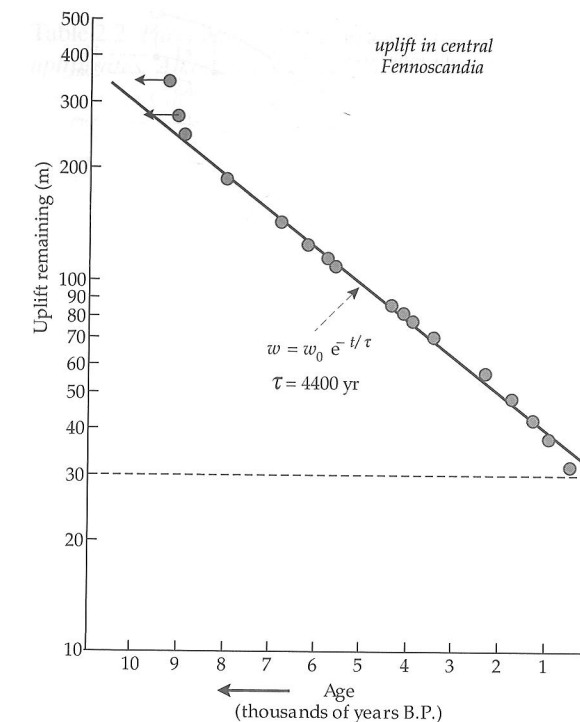


Fig. 2.81 Uplift in central Fennoscandia since the end of the last ice age illustrates exponential viscous relaxation with a time constant of 4400 yr (after Cathles, 1975).

dimension appropriate to the scale of the load (as will be seen in examples below). A test of these relationships requires data that give surface elevations in the past. These data come from analyses of sea-level changes, present elevations of previous shorelines and directly observed rates of uplift. The ancient horizons have been dated by radiometric methods as well as by sedimentary methods such as varve chronology, which consists of counting the annually deposited pairs of silt and clay layers in laminated sediments. A good example of the exponential restoration of a depressed region is the history of uplift in central Fennoscandia since the end of the last ice age some 10,000 yr ago (Fig. 2.81). If it is assumed that about 30 m of uplift still remain, the observed uplift agrees well with Eq. (2.131) and gives a relaxation time of 4400 yr.

An important factor in modelling uplift is whether the viscous response is caused by the mantle as a whole, or whether it is confined to a low-viscosity layer (or "channel") beneath the lithosphere. Seismic shear-wave velocities are reduced in a low-velocity channel about 100–150 km thick, whose thickness and seismic velocity are however variable from one locality to another. Interpreted as the result of softening or partial melting due to temperatures near the melting point, the seismic low-velocity channel is called the asthenosphere. It is not sharply bounded, yet it must be represented by a distinct layer in viscosity models, which indicate that its viscosity must be at least 25 times less than in the deeper mantle.

The larger the ice-sheet (or other type of surface load), the deeper the effects reach into the mantle. By

studying the uplift following removal of different loads, information is obtained about the viscosity at different depths in the mantle.

2.8.6.1 Viscosity of the upper mantle

About 18,000–20,000 years ago Lake Bonneville, the predecessor of the present Great Salt Lake in Utah, USA, had a radius of about 95 km and an estimated depth of about 305 m. The water mass depressed the lithosphere, which was later uplifted by isostatic restoration after the lake drained and dried up. Observations of the present heights of ancient shorelines show that the central part of the lake has been uplifted by about 65 m. Two parameters are involved in the process: the flexural rigidity of the lithosphere, and the viscosity of the mantle beneath. The elastic response of the lithosphere is estimated from the geometry of the depression that would be produced in isostatic equilibrium. The maximum flexural rigidity that would allow a 65 m deflection under a 305 m water load is found to be about 5×10^{23} N m.

The surface load can be modelled as a heavy vertical right cylinder with radius r , which pushes itself into the soft mantle. The underlying viscous material is forced aside so that the central depression is surrounded by a circular uplifted "bulge." After removal of the load, restorative uplift takes place in the central depression, the peripheral bulge subsides and the contour of zero-uplift migrates outward. The wavelength λ of the depression caused by a load with this geometry has been found to be about 2.6 times the diameter of the cylindrical load. In the case of Lake Bonneville $2r = 192$ km, so λ is about 500 km. The mantle viscosity is obtained by assuming that the response time of the lithosphere was short enough to track the loading history quite closely. This implies that the viscous relaxation time τ must have been 4000 yr or less. Substitution of these values for λ and τ in Eq. (2.132) suggests a maximum mantle viscosity η of about 2×10^{20} Pa s in the top 250 km of the mantle. A lower value of η would require a thinner low-viscosity channel beneath the lithosphere.

The Fennoscandian uplift can be treated in the same way (Fig. 2.82), but the weight and lateral expanse of the load were much larger. The ice-cap is estimated to have been about 1100 m thick and to have covered most of Norway, Sweden and Finland. Although the load was therefore somewhat elongate, it is possible to model it satisfactorily by a vertical cylinder of radius $r = 550$ km centered on the northern Gulf of Bothnia (Fig. 2.83). The load was applied for about 20,000 yr before being removed 10,000 yr ago. This caused an initial depression of about 300 m, which has subsequently been relaxing (Fig. 2.82). The uplift rates allow upper-mantle viscosities to be estimated. The data are compatible with different models of mantle structure, two of which are compared in Fig. 2.83. Each model has an elastic lithosphere with a flexural rigidity of 5×10^{24} N m underlain by a low-viscosity channel

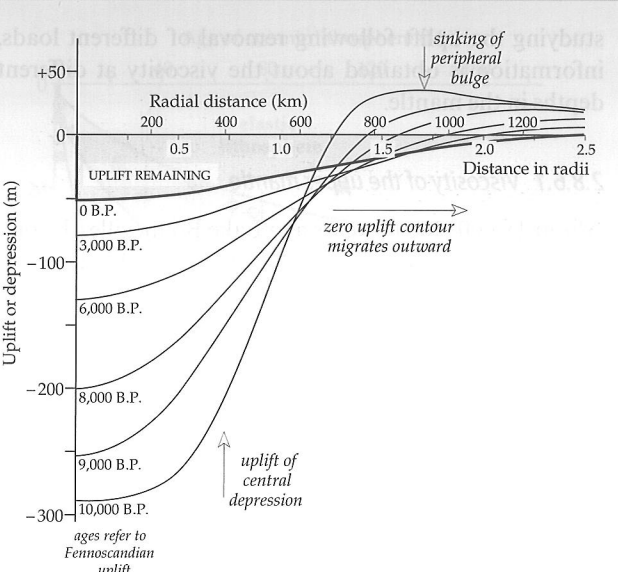


Fig. 2.82 Model calculations of the relaxation of the deformation caused by the Fennoscandian ice-sheet following its disappearance 10,000 yr ago (after Cathles, 1975).

Model 1:		Model 2:	
lithosphere:	$D = 5 \times 10^{24}$ N m	lithosphere:	$D = 5 \times 10^{24}$ N m
low viscosity channel:		low viscosity channel:	
thickness = 75 km		thickness = 100 km	
$\eta = 4 \times 10^{19}$ Pa s		$\eta = 1.3 \times 10^{19}$ Pa s	
mantle:	$\eta = 10^{21}$ Pa s		

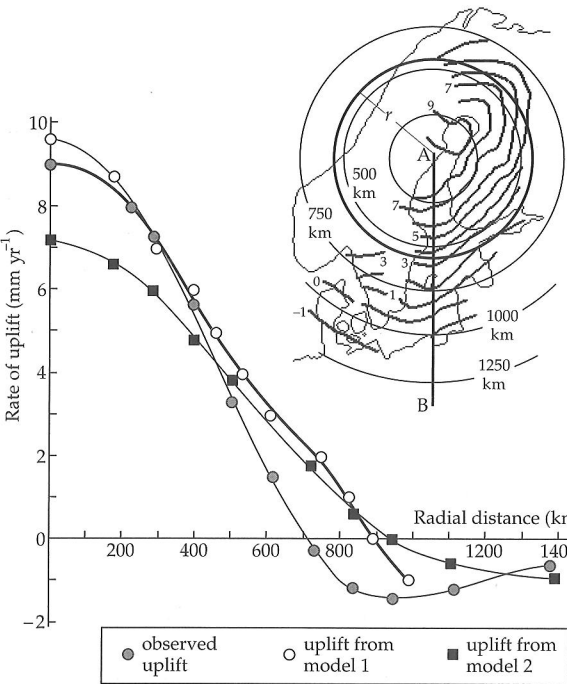


Fig. 2.83 Comparison of Fennoscandian uplift rates interpreted along profile AB (inset) with uplift rates calculated for two different models of mantle viscosity, assuming the ice-sheet can be represented by a vertical right cylindrical load centered on the northern Gulf of Bothnia (after Cathles, 1975).

and the rest of the mantle. The first model has a 75 km thick channel ($\eta = 4 \times 10^{19}$ Pa s) over a viscous mantle ($\eta = 10^{21}$ Pa s). The alternative model has a 100 km thick channel (viscosity coefficient $\eta = 1.3 \times 10^{19}$ Pa s) over a

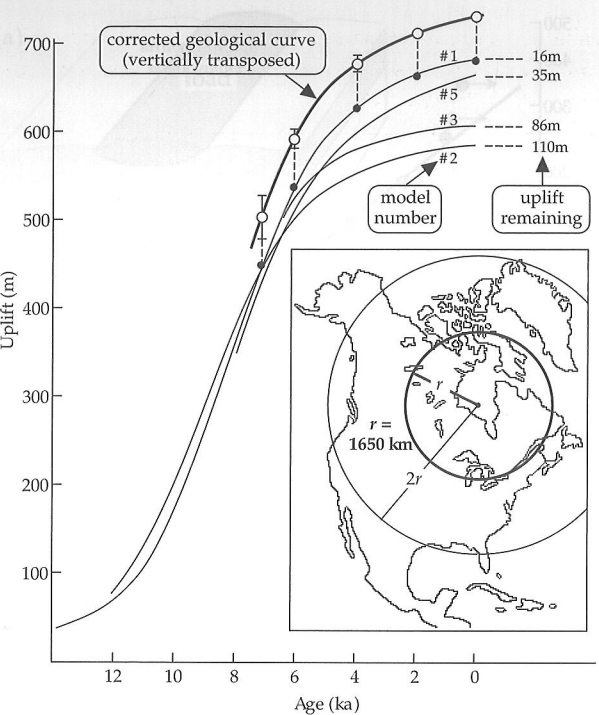


Fig. 2.84 Comparison of uplift history in the James Bay area with predicted uplifts for various Earth models after disappearance of the Wisconsin ice-sheet over North America, represented as a vertical right cylindrical load with radius 1650 km as in the inset (after Cathles, 1975). For details of model parameters see Table 2.2.

rigid mantle. Both models yield uplift rates that agree quite well with the observed uplift rates. However, results from North America indicate that the lower mantle is not rigid and so the first model fits the data better.

2.8.6.2 Viscosity of the lower mantle

Geologists have developed a coherent picture of the last glacial stage, the Wisconsin, during which much of North America was covered by an ice-sheet over 3500 m thick. The ice persisted for about 20,000 yr and melted about 10,000 yr ago. It caused a surface depression of about 600 m. The subsequent history of uplift in the James Bay area near the center of the feature has been reconstructed using geological indicators and dated by the radiocarbon method (see Section 4.1.4.1). For modelling purposes the ice-sheet can be represented as a right cylindrical load with radius $r = 1650$ km (Fig. 2.84, inset). A load as large as this affects the deep mantle. The central uplift following removal of the load has been calculated for several Earth models. Each model has elastic parameters and density distribution obtained from seismic velocities, including a central dense core. The models differ from each other in the number of viscous layers in the mantle and the amount by which the density gradient departs from the adiabatic gradient (Table 2.2). The curvature of the observed uplift curve only fits models in which the viscosity of the lower mantle is around 10^{21} Pa s (Fig. 2.84).

A highly viscous lower mantle ($\eta = 10^{23}$ Pa s, model 4) is

2.9 SUGGESTIONS FOR FURTHER READING

Table 2.2 Parameters of Earth models used in computing uplift rates. All models are for an elastic Earth with a dense core (after Cathles, 1975)

Model	Density gradient	Viscosity [10^{21} Pa s]	Depth interval
1	adiabatic	1	entire mantle
2	adiabatic, except 335–635 km	1	entire mantle
3	adiabatic, except 335–635 km	0.1	0–335 km
4	adiabatic	100	335 km to core
5	adiabatic	1	0–985 km
		2	985–2185 km
		3	2185 km to core

incompatible with the observed uplift history. The best fit is obtained with model 1 or 5. Each has an adiabatic density gradient, but model 1 has a uniform lower mantle with viscosity 10^{21} Pa s, and model 5 has η increasing from 10^{21} Pa s below the lithosphere to 3×10^{21} Pa s just above the core.

The viscoelastic properties of the Earth's interior influence the Earth's rotation, causing changes in the position of the instantaneous rotation axis. The motion of the axis is traced by repeated photo-zenith tube measurements, in which the zenith is located by photographing the stars vertically above an observatory. Photo-zenith tube measurements reveal systematic movements of the rotation axis relative to the axis of the figure (Fig. 2.85). Decomposed into components along the Greenwich meridian (X -axis) and the 90°W meridian (Y -axis), the polar motion exhibits a fluctuation with cyclically varying amplitude superposed on a linear trend. The amplitude modulation has a period of approximately seven years and is due to the interference of the 12-month annual wobble and the 14-month Chandler wobble. The linear trend represents a slow drift of the pole toward northern Canada at a rate of 0.95 degrees per million years. It is due to the melting of the Fennoscandian and Laurentide ice-sheets. The subsequent uplift constitutes a redistribution of mass which causes modifications to the Earth's moments and products of inertia, thus affecting the rotation.

The observed polar drift can be modelled with different viscoelastic Earth structures. The models assume a 120 km thick elastic lithosphere and take into account different viscosities in the layers bounded by the seismic discontinuities at 400 km and 670 km depths (Section 3.7, Table 3.4) and the core–mantle boundary. An Earth that is homogeneous below the lithosphere (without a core) is found to give imperceptible drift. Inclusion of the core, with a density jump across the core–mantle boundary and assuming the mantle viscosity to be around 1×10^{21} Pa s, gives a drift that is perceptible but much slower than that

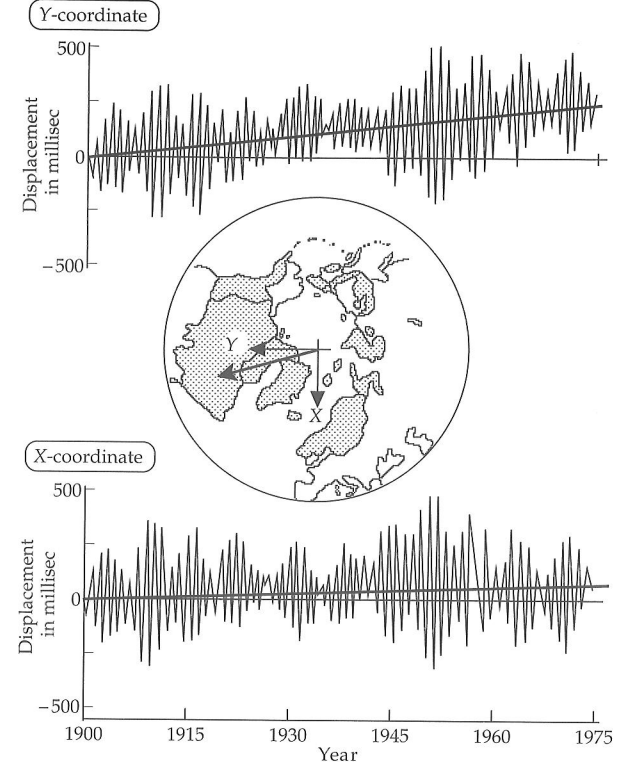


Fig. 2.85 Changes in the position of the instantaneous rotation axis from 1900 to 1975 relative to axes defined in the inset (after Peltier, 1989).

observed. Introduction of a density change at the 670 km discontinuity increases the drift markedly; the 400 km discontinuity does not noticeably change the drift further. The optimum model has an upper-mantle viscosity of about 1×10^{21} Pa s and a lower-mantle viscosity of about 3×10^{21} Pa s. The model satisfies both the rate of drift and its direction (Fig. 2.85). The viscosities are comparable to values found by modelling post-glacial uplift (Table 2.2, model 5).

2.9 SUGGESTIONS FOR FURTHER READING

Introductory level

- Kearey, P., Brooks, M. and Hill, I. 2002. *An Introduction to Geophysical Exploration*, 3rd edn, Oxford: Blackwell Publishing.
- Massonnet, D. 1997. Satellite radar interferometry. *Sci. Am.*, **276**, 46–53.
- Mussett, A. E. and Khan, M. A. 2000. *Looking into the Earth: An Introduction to Geological Geophysics*, Cambridge: Cambridge University Press.
- Parasnis, D. S. 1997. *Principles of Applied Geophysics*, 5th edn, London: Chapman and Hall.
- Sharma, P. V. 1997. *Environmental and Engineering Geophysics*, Cambridge: Cambridge University Press.